MODELLING THE EFFECT OF INJECTION PRESSURE ON HEAT RELEASE PARAMETERS AND NITROGEN OXIDES IN DIRECT INJECTION DIESEL ENGINES

by

Levent YUKSEK *, Tarkan SANDALCI, Orkun OZENER, and Alp Tekin ERGENC

Automotive Sub-Division, Mechanical Engineering Department, Yildiz Technical University, Istanbul, Turkey

Original scientific paper
DOI: 10.2298/TSCI121220101Y

Investigation and modelling the effect of injection pressure on heat release parameters and engine-out nitrogen oxides are the main aim of this study. A zero-dimensional and multi-zone cylinder model was developed for estimation of the effect of injection pressure rise on performance parameters of diesel engine. Double-Wiebe rate of heat release global model was used to describe fuel combustion. Extended Zeldovich mechanism and partial equilibrium approach were used for modelling the formation of nitrogen oxides. Single cylinder, high pressure direct injection, electronically controlled, research engine bench was used for model calibration. 1000 and 1200 bar of fuel injection pressure were investigated while injection advance, injected fuel quantity and engine speed kept constant. The ignition delay of injected fuel reduced 0.4 crank angle with 1200 bar of injection pressure and similar effect observed in premixed combustion phase duration which reduced 0.2 crank angle. Rate of heat release of premixed combustion phase increased 1.75% with 1200 bar injection pressure. Multi-zone cylinder model showed good agreement with experimental in-cylinder pressure data. Also it was seen that the NO_x formation model greatly predicted the engine-out NO_x emissions for both of the operation modes.

Key words: *Wiebe rate of heat release, multi-zone model, nitrogen oxide formation model, injection pressure, diesel engine combustion*

Introduction

Diesel engines have considerable advantages in the aspect of engine power, fuel economy and durability. They were widely applied in heavy-duty vehicles, also diesel engines have a great market share in small vehicles today [1]. Technological improvement of precise control technology with high pressure injection allows for a better control of combustion which is the source of pollutant emissions and diesel engine noise. European Parliament has mandated the further reduction of nitrogen oxides (NO_x) in Euro-6 emission legislations [2]. Common-rail high pressure injection systems provide drastic reduction in engine-out emissions, with low consumption of fuel and reduced level of combustion noise [3-8]. In order to meet increasing environmental concerns and more stringent emission regulations, current researches are carried out aiming the reduction of emissions simultaneously while maintaining reasonable fuel economy and engine power [9-11].

* Corresponding author; e-mail: lyuksek@yildiz.edu.tr

Modelling the physical processes of an internal combustion engine is one of the indispensable applications which provides adequate knowledge about the non-experienced test points and reduces the number of necessary experimental tests, which means lower developing cost. Engine models mainly constructed upon the mass, momentum and energy conservation equations. Accuracy of the outputs depends on the complexity of the model. Dimensionless single-zone models need lower computational times while maintaining satisfactory results for overall engine parameters and emission investigations [12]. Quasi-dimensional or so called multi-zone models are dividing cylinder into several sub-zones which interact with each other. The multi-zone models give better accuracy for combustion analysis due to the mass and heat transfer between constituent zones [13]. Neither single zone, nor multi-zone models can simulate the spatial distribution of chemical species. Computational fluid dynamic applications are capable of modelling in-cylinder turbulence, spray penetration, combustion, and emission formation but spatial computation needs high computational time [14, 15].

The single-zone and the multi-zone models are relatively easy applications to develop and are optimum to operate, generally they only use conservation equations and neglect the behaviour of in-cylinder motion of the charge and detailed spray physics [12, 16]. The combustion phenomenon is calculated via the mathematical definition of the rate of heat release (ROHR) in these types of dimensionless models such as Wiebe functions [17, 18]. Several other simplification approaches or assumptions such as heat transfer and blow-by sub-models are well implemented in dimensionless simulations [19]. In order to calculate the rate of emissions, kinetic calculations can be added to dimensionless models, the complexity of kinetic model mainly determines the simulation time and accuracy of engine out emission predictions [20]. With implementing kinetic models NO_x, unburned hydrocarbons, CO and CO_2 emissions can be modelled precisely [21, 22]. Nitrogen oxide kinetic is relatively slow when compared to hydrocarbon kinetic reactions, also nitrogen oxides keep formation out of the flame area, for these reasons NO_x formation rates can be calculated with a separate mechanism which so-called as Zeldovich mechanism [23].

Aim of this study is to model the effect of increased fuel injection pressure on ROHR Wiebe parameters and NO_x emissions. A dimensionless, multi-zone thermodynamic model was developed based upon first law of thermodynamics and conservation of mass. Several sub-models implemented to calculate separate events such as the flows through valves, heat transfer, blow-by and injection. Model outputs validated with experimental results which obtained from a high pressure injection capable single cylinder research engine.

Details of thermodynamic model

This section gives a description of the main hypotheses and sub-models on which the thermodynamic model is based.

Basic hypotheses

Below-listed assumptions are made,

(1) Chamber pressure was assumed to be uniform.
(2) Three species were considered which are air, fuel vapour, and combustion products. Temperature dependent specific heats of the species were obtained from JANAF polynomials [24].

(3) Two distinct zones considered which are designated as burned and unburned, mass and energy conservation were considered between zones and zone temperature and volumes calculated with respect to crank angle degree (CAD).
(4) Perfect gas behaviour was assumed to ease the calculation process.
(5) Charge internal energy was calculated assuming bulk temperature in the chamber.
(6) Heat transfer to the chamber walls was considered. Both convective and radiative heat transfer were calculated during cycle simulation.
(7) Blow-by leakage was considered.
(8) Simulation of fuel injection consists of the calculation of characteristic break-up time, instantaneous Sauter mean diameter (SMD) and heat of vaporisation according to the model developed by Hiroyasu *et al.* [25].
(9) An empirical combustion model was applied.

Model structure and sub-models

Entire model consists of four different stroke models and distinguishes each other with valve timings. The energy and mass balances were solved between 1-720 CAD, considering the combustion chamber as an open system due to the fuel injection, the inlet and exhaust of the charge and blow-by leakage through boundaries. The main results are the instantaneous pressure and temperature for compression and expansion strokes while the mass flow was also calculated during intake and exhaust strokes. According to the hypotheses 1, no spatial resolution of the thermodynamic properties was considered. Overall balance equation which applied in every CAD of simulation consists of the first law of thermodynamics for an open system as stated in eq. (1). Differentiating the eq. (1) respect to CAD yields the eq. (2) which determines the general ordinary differential equation of the model. Figure 1 indicates the open system approach which the formulations depending on:

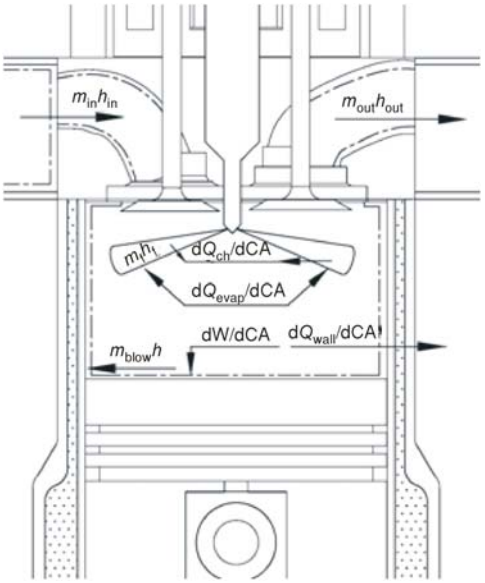

Figure 1. Overall energy balance of internal combustion engine

$$Q - W = \Delta U_{\text{cyl}} + (m_{\text{in}}h_{\text{in}} - m_{\text{out}}h_{\text{out}} - m_{\text{blow}}h + m_{\text{f}}h_{\text{f}}) \tag{1}$$

$$\left(\frac{\mathrm{d}Q_{\text{ch}}}{\mathrm{d}\theta} - \frac{dQ_{\text{wall}}}{\mathrm{d}\theta} - \frac{dQ_{\text{evap}}}{\mathrm{d}\theta}\right) - p\frac{\mathrm{d}V}{\mathrm{d}\theta} = \frac{U_{\text{cyl}}}{\mathrm{d}\theta}\frac{\mathrm{d}}{\mathrm{d}\theta}(m_{\text{in}}h_{\text{in}} - m_{\text{out}}h_{\text{out}} - m_{\text{blow}}h + m_{\text{f}}h_{\text{f}}) \tag{2}$$

Thermophysical properties of the working fluid such as the specific heat and the enthalpy were computed using polynomials in eqs. (3) and (4). Mass transferred from ring crevices through the crankcase is obtained by applying the model developed by Petris *et al*. [26]:

$$\frac{C_{p,k}}{R_{\text{ideal}}} = a_{1,k} + a_{2,k}T + a_{3,k}T^2 + a_{4,k}T^3 + a_{5,k}T^4 \tag{3}$$

$$C_{\mathrm{v,k}} = C_{p,k} - R_{\mathrm{ideal}} \tag{4}$$

Cylinder volume sub-model

The instantaneous cylinder volume was calculated according to piston motion equation [27] in eq. (5) and eq. (6):

$$V_{\mathrm{c}} = V_{\mathrm{tot}} - V_{\mathrm{disp}} \tag{5}$$

$$V(\theta) = V_{\mathrm{c}} + \frac{\pi D^2}{4} R\left[(1-\cos\theta) + \frac{\lambda}{4}(1-\cos 2\theta)\right] \tag{6}$$

Adiabatic flame temperature sub-model

Burned zone and unburned zone gas temperatures were calculated by using the ideal gas equation of the state in eq. (7) which was also necessary for the determination of specific heat of medium. During the combustion period, flame temperature reaches maximum value when conditions assumed to be adiabatic and radiative heat transfer depends on the flame temperature in burned-zone. Difference between the flame temperature and the average temperature is the main reason of the errors in heat transfer calculations. In order to calculate the temperature of the flame, molar concentrations of the species were obtained according to the combustion stoichiometry as described in eq. (8):

$$T(\theta) = \frac{P(\theta)V(\theta)}{m_{\mathrm{intake}} R_{\mathrm{ideal}}} \tag{7}$$

$$\mathrm{C_xH_y} + \left(x + \frac{y}{4}\right)(\mathrm{O_2} + 3.773\mathrm{N_2}) = x\mathrm{CO_2} + \frac{y}{2}\mathrm{H_2O} + 3.773\left(x + \frac{y}{4}\right)\mathrm{N_2} \tag{8}$$

The adiabatic flame temperature was determined according to the Borman [28] by applying iterative solution for eq. (9):

$$\Sigma h_{\mathrm{reactants}} = \Sigma h_{\mathrm{products}} \tag{9}$$

Heat transfer sub-model

Annand's heat transfer model [19] was used to calculate the instantaneous wall heat transfer, which considers both convection and radiation heat transfer as indicated in eq. (10). Where the h_{c} is the convection heat transfer coefficient and defined by the author as eq. (11). The average cylinder temperature was used for the calculation of non-combustion period heat transfer when the radiation heat transfer is negligible. The adiabatic flame temperature in burned zone was used to calculate radiation heat transfer during combustion period:

$$Q_{\mathrm{total}} = h_{\mathrm{c}} A_{\mathrm{ht}} (T_{\mathrm{g}} - T_{\mathrm{w}}) + \beta\sigma(T_{\mathrm{g}}^4 - T_{\mathrm{w}}^4) \tag{10}$$

$$\frac{h_{\mathrm{c}} D}{k_{\mathrm{an}}} = a_{\mathrm{an}}\left(\frac{\rho_{\mathrm{a}} C_m D}{\mu}\right)^{b_{an}} \tag{11}$$

Fuel injection sub-model

Injected fuel quantity per crank angle was calculated according to eq. (12). Discharge coefficient of the nozzle was determined by the series of laboratory experiments. Fuel injection quantity per given signal length was measured hence the nozzle rise time and the discharge coefficient was obtained:

$$\frac{\mathrm{d}Q_{\mathrm{flow}}}{\mathrm{d}\theta} = \sqrt{2\Delta P_{\mathrm{inj}}\rho_{\mathrm{f}}}\, A_{\mathrm{inj}} Cd \frac{\mathrm{d}t}{\mathrm{d}\theta} \tag{12}$$

Characteristic break-up time, instantaneous SMD and evaporation rate of injected fuel package were calculated with using eq. (13) and eq. (14) according to Hiroyasu *et al.*:

$$t_{\mathrm{break}} = 28.65 \frac{\rho_{\mathrm{f}} d_{\mathrm{noz}}}{\sqrt{\rho_{\mathrm{a}} \Delta p_{\mathrm{in\,j}}}} \tag{13}$$

$$SMD = 23.9\mathrm{e}^{-6} \Delta p_{\mathrm{in\,j}}^{-0.135} \rho_{\mathrm{a}}^{0.12} m v_{\mathrm{in\,j}}^{0.131} \tag{14}$$

Valve mass flow sub-model

Mass flow from valves during intake and exhaust strokes was calculated by using compressible flow equations adopted by Bowler [29]. Author indicated that the effective mass flow area of a poppet valve varies depending on the valve lift and can be categorized as three main cases. After defining the effective mass flow area, the total mass flow can be calculated according to eq. (16) and eq. (17) depending on the ratio of flow velocity to sound speed in the choke region. If the flow is choked which can be determined by eq. (15) than the mass flow can be calculated by using eq. (16), for the non-choked conditions mass flow can be calculated with eq. (17):

$$\frac{P_{\mathrm{T}}}{P_0} \le \left(\frac{2}{k+1}\right)^{\frac{k}{k-1}} \tag{15}$$

$$Q_{\mathrm{valve}} = \frac{C_{\mathrm{D}} A_{\mathrm{m}} P_0}{\sqrt{R_{\mathrm{ideal}} T_0}} \sqrt{k} \left(\frac{2}{k+1}\right)^{\frac{k+1}{2(k-1)}} \tag{16}$$

$$Q_{\mathrm{valve}} = \frac{C_{\mathrm{D}} A_{\mathrm{m}} P_0}{\sqrt{R_{\mathrm{ideal}} T_0}} \left(\frac{P_{\mathrm{T}}}{P_0}\right)^{1/k} \sqrt{\frac{2k}{k-1}\left[1 - \left(\frac{P_{\mathrm{T}}}{P_0}\right)^{\frac{k-1}{k}}\right]} \tag{17}$$

Rate of heat release sub-model

Engine combustion process was modelled by using the double-Wiebe ROHR curves which offered by Miyamoto *et al*. [18]. Considering the original equation of Wiebe [17], Miyamoto developed combined model for the combustion of diesel engines. Double Wiebe takes into account both of the combustion phases that named as mixture controlled and diffusion controlled phases. Equations (18) and (19) are the mathematical description of premixed and diffusive combustion phases respectively. Total rate of heat release is the sum of both curves as described in eq. (20):

$$\frac{\mathrm{d}Q_{\mathrm{p}}}{\mathrm{d}\theta} = \frac{Q_{\mathrm{p}}}{\theta_{\mathrm{p}}} a(m_{\mathrm{p}}+1)\left(\frac{\theta-\theta_0}{\theta_{\mathrm{p}}}\right)^{m_p} \mathrm{e}^{-a\left(\frac{\theta-\theta_0}{\theta_p}\right)^{m_p+1}} \tag{18}$$

$$\frac{\mathrm{d}Q_{\mathrm{d}}}{\mathrm{d}\theta} = \frac{Q_{\mathrm{d}}}{\theta_{\mathrm{d}}} a(m_{\mathrm{d}}+1)\left(\frac{\theta-\theta_0}{\theta_{\mathrm{d}}}\right)^{m_p} \mathrm{e}^{-a\left(\frac{\theta-\theta_0}{\theta_d}\right)^{m_d+1}} \tag{19}$$

$$\frac{\mathrm{d}Q}{\mathrm{d}\theta} = \frac{\mathrm{d}Q_{\mathrm{p}}}{\mathrm{d}\theta} + \frac{\mathrm{d}Q_{\mathrm{d}}}{\mathrm{d}\theta} \tag{20}$$

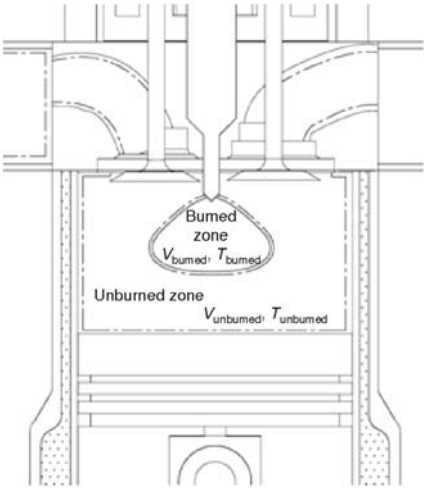

Figure 2. Regions of two-zone model

Empirical two zone combustion model

Estimation of tail-pipe NO_x emissions is not precisely possible without considering the local peak temperatures due to exponential temperature dependence of the chemical reaction mechanism of NO_x. Single zone cylinder models are not capable to calculate combustion product temperatures, in order to overcome this drawback an empirical two zone combustion model which offered by Heider *et al*. [30] is implemented. Authors divided cylinder gases into two separate zones which called the burned and the unburned zones as indicated in fig. 2.

Following assumptions are made for solving the two-zone model statements:

– ideal gas behaviour for both zones was assumed.
– zones were isolated between them by infinite-thin boundary film.
– Conservation of mass and energy were considered between zones.
– Heat of reaction was completely released in burned zone.
– Equivalence ratio in burned zone was approximately unity.

Conservation of mass was considered with applying eq. (21) while the instantaneous cylinder volume is the sum of burned and unburned zone volumes as described in eq. (22). Pressure of zones was assumed to be same and equal to the in-cylinder pressure:

$$m_{\text{unburned}} + m_{\text{burned}} = m_{\text{intake}} \tag{21}$$

$$V_{\text{unburned}} + V_{\text{burned}} = V \tag{22}$$

Mass of the burned zone was calculated as the sum of burned fuel mass and air required for the combustion with stoichiometric equivalence ratio as described in eq. (23), unburned zone mass was calculated with using eq. (21):

$$m_{\text{burned}} = m_{\text{f}}(\alpha f_{\text{stoich}} + 1) \tag{23}$$

Conservation equation of energy of total system was solved for the calculation of zone temperatures, specific heats of zone mediums were considered as equal for the simplification hence conservation equation simplified to form written in eq. (24):

$$m_{\text{unburned}} T_{\text{unburned}} + m_{\text{burned}} T_{\text{burned}} = m_{\text{intake}} T \tag{24}$$

$$V_{\text{burned}} = \frac{m_{\text{burned}} R_{\text{ideal}} T_{\text{burned}}}{P} \tag{25}$$

Solving the temperature and the mass of distinct zones with respect to CAD, makes it possible to calculate the zonal volumes with using ideal gas equation of state in eq. (25).

NO_x formation model

Thermal NO formation mechanism first offered by Zeldovich [31] and it was extended by Lavoie *et al.* [23] and Baulch *et al*. [32]. Thermal NO_x formation mechanisms consist of three

elementary reactions which were used for the estimation of engine out NO_x emissions in this study:

$$N_2 + O \xleftrightarrow{k_1} NO + N \tag{26}$$

$$O_2 + N \xleftrightarrow{k_2} NO + O \tag{27}$$

$$OH + N \xleftrightarrow{k_3} H + NO \tag{28}$$

Equations (26)-(28) are the skeletal mechanism of NO_x model. Rate of reactions are kinetically controlled and have strong dependence on temperature. Rate constants of NO_x model are given in form of the Arrhenius equation described as $ATexp(-Ea/T)$, and listed in tab. 1. Forward and reverse rate constants were adopted into the NO_x model from the study of Hanson *et al.* [33].

Table 1. Reaction rate constants of NO_x chemistry model (in units of cm^3, gmol, s, K)

	Reaction	Forward rate constant	Reverse rate constant
1	$N_2 + O \xleftrightarrow{k_1} NO + N$	$1.8E14\exp(-38370/T)$	$3.8E13\exp(-425/T)$
2	$O_2 + N \xleftrightarrow{k_2} NO + O$	$1.8E10T\exp(-4680/T)$	$3.81E9T\exp(-20820/T)$
3	$OH + N \xleftrightarrow{k_3} H + NO$	$7.1E13\exp(-450/T)$	$1.7E14\exp(-4560/T)$

Partial equilibrium approach for the [O] and [OH] was considered. Rate of NO_x model reactions were calculated respect to CAD with considering the burned-zone temperature.

Methodology of ROHR regression

Non-linear multiple independent variable regression was implemented for determination of Wiebe coefficients. Matlab software was used for programming the regression. Goodness of each regression is estimated by a coefficient of determination which so called R^2 value in statistics. Solution of non-linear regression was made by using Gauss-Newton method where the intended coefficient of determination is 0.99. Initial values of m_p and m_d were set to 5 for each of Wiebe parameter, upper and lower limits was set to 50 and 0.1, respectively. Values higher than 50 indicate infinitesimally fast combustion which can not be occurred in real conditions.

Experimental set-up and methodology

The parameter adjustment process for the different sub-models is necessary due to the differences in test engines which mainly the result of the discrepancies of the combustion systems. In this study, validation of the model outputs for a better parameter adjustment was done with experimental data obtained from a diesel test engine. The experimental measurements were carried out on a single cylinder, high-speed direct-injection research diesel engine with 0.45 litre of displacement volume. Specifications of test engine are listed in tab. 2.

The engine was directly coupled to a DC electric dynamometer which controlled by a computer. Engine speed and position were measured with an incremental encoder that has resolution of 0.1 CAD. In-cylinder pressure measurements were carried out with a Kistler 6052 B piezoelectric pressure sensor, Kistler 5011 B charge amplifier, and a LeCroy wave surfer 24Xs 4 channel digital oscilloscope. In order to reduce the effect of cyclic variations 50 consecutive cy-

cle data were logged than averaged. Nitrogen oxides were measured with AVL Dicom 4000 gas analyser. Scheme of the test system is shown in fig. 3., also accuracies of the measurements and uncertainties of derived variables are listed in tab. 3, which were calculated according to Kline and McClintock [34].

Table 2. Technical specifications of test engine

Specification	Unit	Value
Total displacement volume	cm^3	454
Number of cylinders	–	1
Stroke length	mm	80
Bore	mm	85
Compression ratio	–	17.5:1
Number of intake valves	–	1
Number of exhaust valves	–	1
Intake valve opening	CA deg.	21° bTDC
Intake valve closing	CA deg.	38° aBDC
Exhaust valve opening	CA deg.	46° bBDC
Exhaust valve closing	CA deg.	21° aTDC

Table 3. Accuracies of the measurements and the uncertainties in the calculated results

Measured parameter	Measurement device	Accuracy
Engine torque	Load cell	± 0.5%
Engine speed	Incremental encoder	±1 rpm
NO_x	AVL Dicom 4000	1 ppm
Fuel flow rate	Sartorius BP 211D	±0.25%
In-cylinder pressure	Kistler 6052 B	± 0.3%
Calculated results		Uncertainty
Indicated power		±0.35%
Brake power		±0.55%
ISFC		±0.6%
BSFC		±0.8%

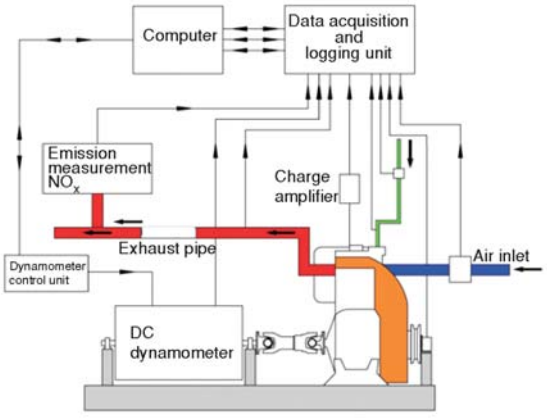

Figure 3. Schematic of the test bench

Fuel injection system of the test engine was upgraded to electronically controlled high pressure injection structure from a mass production engine. Entire system consists of an injection pump, a rail, a relieve valve, a pressure sensor, and finally, a sac type nozzle injector. Schematic view of assembly of injection system is shown in fig. 4. The injection system is capable to vary injection pressure between 200 to 1800 bar, injection pressure was set *via* release valve on rail. The selected rail capacity was large enough to compensate possible pressure fluctuations hence the injection pressure kept constant during injection. Fuel is injected into the cylinder in direct-injection engines both for diesel and gasoline types. Considering the ideal conditions for maximizing the cycle efficiency, fuel heat must be released infinitesimally short duration at TDC according to thermodynamics. While in real engine conditions it is not possible due to necessity of time for initialisation and progression of

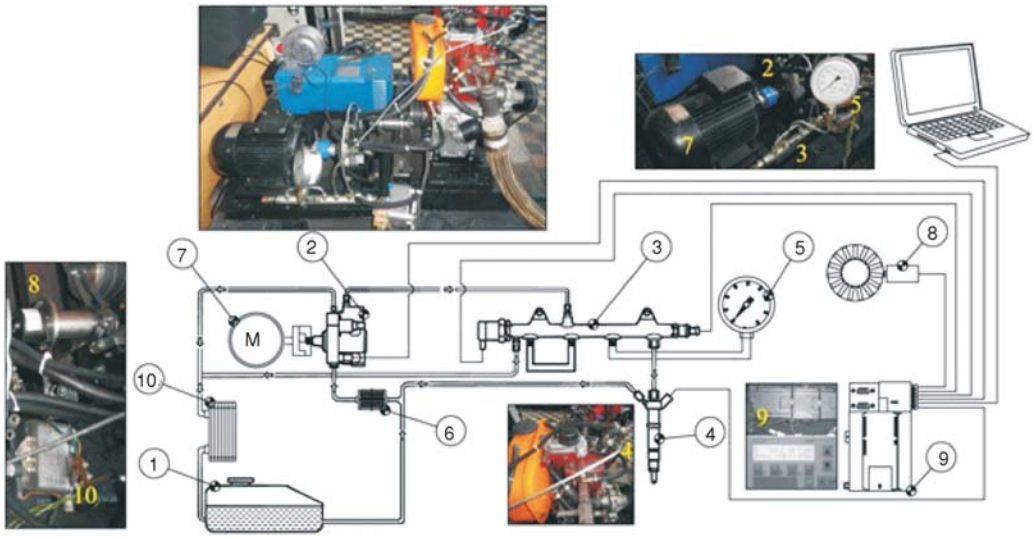

Figure 4. Schematic of the fuel injection system
1 – Fuel tank, 2 – high pressure pump, 3 – rail, 4 – injector, 5 – manometer, 6 – fuel filter, 7 – AC motor, 8 – encoder, 9 – PLC, 10 – heat ecxhanger

combustion. Therefore in order to provide enough time to related preparation process, injection is made with a time advance BTDC which is so called injection advance. A Siemens branded PLC was used to facilitate injection signals, where the data collected from the encoder was processed to set injection time precisely. Computer based programming interface was used to enter fuel injection advance and quantity per cycle.

Effect of injection pressure on engine performance outputs were investigated by injecting equal amount of fuel both in high and low pressure injection scenarios while engine speed were kept constant. Engine power, brake specific fuel consumption (BSFC), in-cylinder pressure, NO_x emissions were measured at steady-state conditions. Details of test conditions are summarized in tab. 4.

Table 4. Details of test conditions

Designation	P1000	P1200
Injection pressure [bar]	1000	1200
Engine speed [rpm]	2000	2000
Injected fuel quantity [mg per cycle]	26	26
Injection advance CAD	15°	15°

Results

Engine performance and NO_x

Generally, high pressure injection results in smaller spray droplets and shorter injection periods. The well atomized spray shortens the ignition delay, it is commonly believed that the benefit of high injection pressure is the reduction of particulate matter and the injection timing can be retarded as to reduce NO_x. There was no performance improvement observed with P1200 mode, where the measurements were in the range of system uncertainty. According to in-cylinder pressure measurements, increased injection pressure affected the combustion parameters as shown in figs. 5 and 6. Ignition delay is defined in literature as a time be-

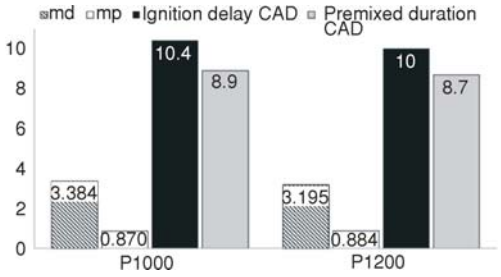

Figure 5. Effect of injection pressure on Wiebe parameters and ignition delay

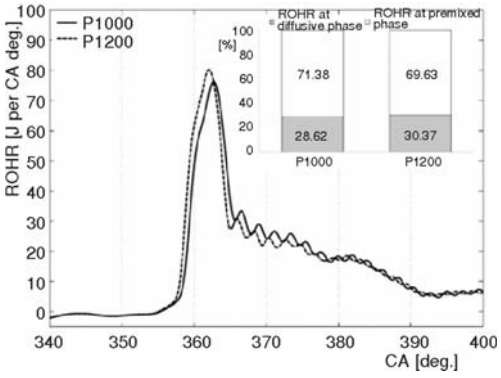

Figure 6. Effect of injection pressure on ROHR of combustion phases

tween the start of injection and start of combustion, both of which have to be measured separately [35]. In current study, start of injection time is considered as the time when the signal created by PLC, delay between the signal and the actual rise of the needle wasn't taken into consideration. Start of combustion is determined via ROHR curve. The ignition delay of injected fuel reduced 0.4 CAD with P1200 operation mode and similar effect observed in premixed combustion phase duration which reduced 0.2 CAD. The ignition delay of the test engine is relatively high when compared to modern common rail diesel engines; this can be attributed to rather old combustion chamber design which was optimised for in-line pump nozzle system. ROHR of premixed combustion phase increased 1.75% with P1200 operation mode.

Obtained results indicate the occurrence of shorter mixture formation duration which possibly is the consequence of the increase of spray penetration. Lower delay of ignition caused an early pressure rise in P1200 mode, also higher ROHR in premixed combustion resulted higher maximum in-cylinder pressure as shown in fig. 7. ROHR of P1200 and P1000 with respect to CAD are shown in fig. 6, where the initiation of combustion of P1200 is earlier while the peak reached to higher values when compared to P1000. Early pressure rise and consequent bulk temperature increase leaded higher NO_x emission in P1200 operation mode, 10.5% increase observed in engine-out NO_x emissions as noted in fig. 7. Despite the lower duration of ignition delay and higher ROHR peak in P1200 operation mode, there were no considerable difference observed in maximum in-cylinder bulk temperatures while rise of P1200 was earlier than P1000. From the view of this point it can be concluded that the early temperature rise also has a significant impact on thermal NO_x formation.

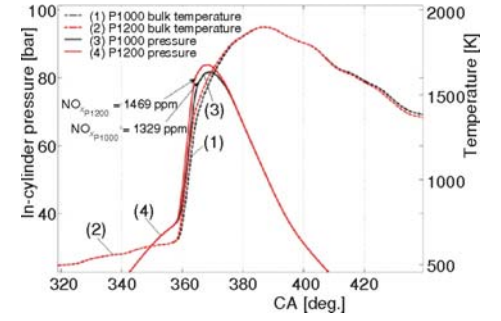

Figure 7. Effect of injection pressure on in-cylinder pressure and bulk temperature

Model outputs

Model parameters were adjusted to satisfy the experimental measurements which were mainly the heat transfer coefficients of Annand heat transfer model, blow-by leakage and ROHR model. Heat transfer in non-combustion phase has to be adjusted exactly for a better estimation of the in-cylinder pressure of the compression stroke. Combustion phase heat transfer mainly constituents of radiation and conduction, where the adiabatic flame temperature be-

comes important for radiation heat transfer. Parameter adjustment study was ended when R^2 value of each regression of experimental data reached 99%, ROHR sub-model outputs were implemented into thermodynamic main model and the final pressure curve was compared with experimental data for validation. Comparison of thermodynamic model results with experimental data are shown in figs. 8 and 9, in spite of being quasi-dimensional of the model constructed in this study, it exposed satisfactory results which are offering an effective solution for in-cylinder pressure estimation.

The model output for the formation of NO_x emissions are shown in fig. 10, for both of P1000 and P1200 operation modes. Single-zone models can not satisfy the accuracy of the NO_x formation due to the assumption of uniform temperature distribution and lack of the differences in concentrations of reaction zones. Therefore multi-zone models are necessary for the modelling of DI diesel NO_x chemistry.

Well-known factor that strongly affect the concentration of engine-out NO_x emissions is the peak temperature of burned zone, while duration of mentioned high temperature region impacts the formation rate as can be concluded from the fig. 10. Variation of the temperature of burned-zone with respect to CAD becomes significant for NO_x formation at around freezing temperatures which the increase in the concentration of NO_x is almost become negligible. One can easily conclude that the duration of high temperature environment is as important as the peak temperature of burned-zone for the formation of NO_x. Nitrogen oxide kinetic model revealed satisfactory results with calculated burned-zone temperatures. Shorter ignition delay and higher ROHR of P1200 successfully simulated with thermodynamic model hence burned zone temperatures and model-out NO_x emissions are in harmony with experimental data.

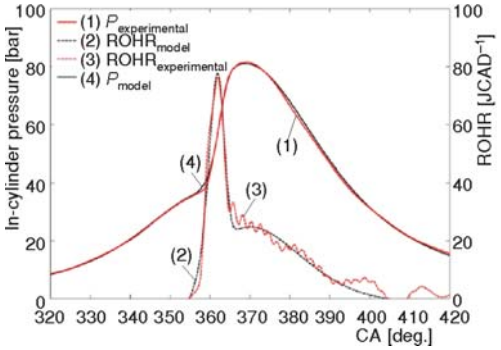

Figure 8. Model results for P1000 operation mode

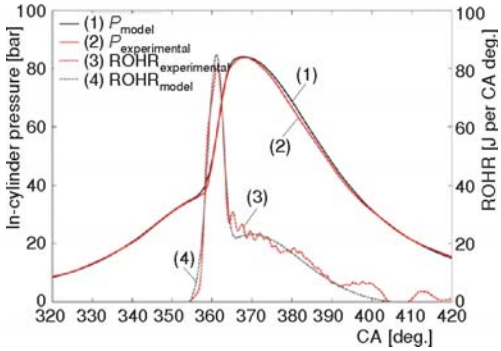

Figure 9. Model results for P1200 operation mode

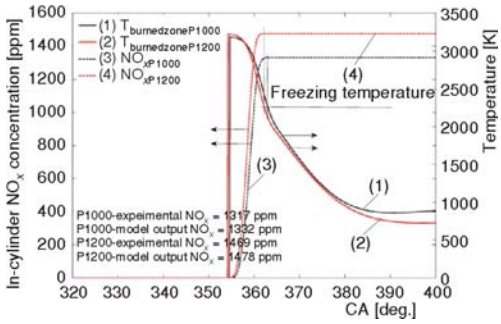

Figure 10. The model output for the formation of NO_x emissions

Conclusions

Aim of this study is to model the effect of increased fuel injection pressure on ROHR parameters and NO_x emissions. A dimensionless, multi-zone thermodynamic model was devel-

oped; model calibration was made with an experimental data obtained from single cylinder, DI diesel engine. An electronically controlled high pressure fuel injection system was adopted on a research engine which can vary injection pressure between 200 and 1800 bar also it is capable to advance of the injection and number of the injection per cycle simultaneously via a computer. 1000 and 1200 bar of fuel injection pressure were investigated while injection advance, injected fuel quantity and engine speed were kept constant. According to the results of experimental and simulation data, obtained conclusions can be listed as:

- There was no performance improvement observed with P1200 mode, where the measurements were in the range of system uncertainty.
- The ignition delay of injected fuel reduced 0.4 CAD with P1200 operation mode and similar effect observed in premixed combustion phase duration which reduced 0.2 CAD. ROHR of premixed combustion phase increased 1.75% with P1200 operation mode.
- 10.5% increase was observed in engine-out NO_x emissions
- Multi-zone cylinder model estimations reached 99% R^2 while nitrogen oxide kinetic model revealed satisfactory results with calculated burned-zone temperatures.

The developed model can calculate both thermodynamic and kinetic processes in acceptable computing time scales. Computational efficiency of these types of dimensionless models eases the estimation effort of un-experienced parameters for engine developers. Further improvement of the model described in this study will be the integration of a reduced kinetic model instead of partial equilibrium approach in order to consider hydrocarbon chemistry.

Acknowledgment

Authors would like to thank to Professor Dr. Orhan DENIZ for his unforgettable contributions to this study as a supervisor.

Nomenclature

a – Wiebe coefficient
a_{an} – Annand heat transfer coefficient
$a_{fstoich}$ – stoichiometric air/fuel ratio
A – Arrhenius constant
A_{ht} – heat transfer surface area, [m^2]
A_{inj} – cross-sectional area of injector nozzle, [m^2]
A_m – minimum cross-sectional area of valve, – [m^2]
b_{an} – Annand heat transfer coefficient
C_d – discharge coefficient
C_m – mean piston speed, [ms^{-1}]
$C_{v,k}$ – constant volume specific heat, [$kJkg^{-1}K^{-1}$]
$C_{p,k}$ – constant pressure specific heat, [$kJkg^{-1}K^{-1}$]
D – bore, [m]
E_a – activation energy, [$kJmol^{-1}$]
h – enthalpy, [$kJkg^{-1}$]
h_c – convection heat transfer coefficient, [$Wm^{-2}K^{-1}$]
h_f – enthalpy of fuel, [$kJkg^{-1}$]
h_{in} – enthalpy of inducted charge, [$kJkg^{-1}$]
h_{out} – enthalpy of exhausted charge, [$kJkg^{-1}$]
$h_{reactants}$ – enthalpy of reactants, [$kJmol^{-1}$]
$h_{products}$ – enthalpy of products, [$kJmole^{-1}$]
k – adiabatic exponent
k_{an} – thermal conductivity of air, [$Wm^{-1}K^{-1}$]
m_{blow} – blow-by mass, [kg]
m_{burned} – burned zone mass, [kg]
m_d – Wiebe coefficient
m_f – injected fuel quantity, [kg]
m_{in} – inducted charge quantity, [kg]
m_{intake} – inducted total air quantity during intake stroke, [kg]
m_{out} – exhausted charge quantity, [kg]
m_p – Wiebe coefficient
$m_{unburned}$ – unburned zone mass, [kg]
m_{vinj} – injected fuel volume, [m^3]
P – in-cylinder pressure, [kPa]
P_0 – upstream pressure, [kPa]
P_{inj} – injection pressure, [kPa]
PT – downstream pressure, [kPa]
Q – released heat, [kJ]
Q_{ch} – chemically released heat, [kJ]
Q_d – heat released in diffusive combustion phase, [kJ]
Q_{evap} – heat required for fuel evaporation, [kJ]
Q_{flow} – flow rate, [kgs^{-1}]
Q_{wall} – heat transferred to the cylinder wall, [kJ]

Q_p – heat released in diffusive premixed phase, [kJ]
Q_{valve} – flow rate through the valve section, [kgs^{-1}]
R – crank radius, [m]
R_{ideal} – universal gas constant, [kJkg^{-1}K^{-1}]
t – time, [s]
t_{break} – fuel break-up time, [s]
T_0 – upstream temperature, [K]
T – in-cylinder average temperature, [K]
T_{burned} – burned zone temperature, [K]
T_g – gas side temperature, [K]
$T_{unburned}$ – unburned zone temperature, [K]
T_w – wall temperature, [K]
TT – downstream temperature, [K]
U_{cyl} – internal energy of charge, [kJ]
V – instantaneous cylinder volume, [m^3]
V_{burned} – burned zone volume, [m^3]
V_c – clearance volume when piston at TDC, [m^3]
V_{disp} – displacement volume, [m^3]
$V_{unburned}$ – unburned zone volume, [m^3]
V_{tot} – total cylinder volume, [m^3]
W – boundary work, [kJ]
W_{ind} – indicated work, [kJ]

Greek symbols

β – Annand heat transfer coefficient
θ – crank angle, [deg.]
q_0 – start of combustion crank angle
θ_d – combustion duration of diffusive phase
θ_p – combustion duration of premixed phase
λ – ratio of the radius of crank to the connecting rod
μ – dynamic viscosity of air, [kgm^{-1}s^{-1}]
ρ_a – air density, [kgm^{-3}]
ρ_f – fuel density, [kgm^{-3}]
s – Stefan-Boltzman coefficient, [Wm^{-2}K^{-4}]

Abbreviations

aBDC – after bottom dead centre
aTDC – after top dead centre
bBDC – before bottom dead centre
BSFC – brake specific fuel consumption
BTDC – before top dead centre
CAD – crank angle degree
DI – direct injection
ISFC – indicated specific fuel consumption
ROHR – rate of heat release
rpm – revolution per minute
PLC – programmable logic controller
TDC – top dead centre

References

[1] ***, *The Automobile Industry Pocket Guide*, European Automobile Manufacturers Association, www.acea.be
[2] ***, Regulation (EC) No 715/2007, *Official Journal of the European Union*, European Union Parliament, http://eur-lex.europa.eu
[3] Benajes, J., *et al*., Influence of Boost Pressure and Injection Pressure on Combustion Process and Exhaust Emissions in a HD Diesel Engine, SAE technical paper 2004-01-1842, 2004
[4] Bianchi, G.M., *et al*., Numerical Analysis of Passenger Car HSDI Diesel Engines with the 2nd Generation of Common Rail Injection Systems: The Effect of Multiple Injections on Emissions, SAE technical paper 2001-01-1068, 2001
[5] Han, S., Bae, C., The Influence of Fuel Injection Pressure and Intake Pressure on Conventional and Low Temperature Diesel Combustion, SAE technical paper 2012-01-1721,2012
[6] Themel, T., *et al*., Diesel Engine Response to High Fuel-Injection Pressures, SAE paper 982683, 1998
[7] Thirouard, M., *et al*., Potential to Improve Specific Power Using Very High Injection Pressure In HSDI Diesel Engines, SAE technical paper 2009-01-1524,2009
[8] Wen, T., *et al*., Injection Pressure Influence on Diesel Engine Performance and Emissions, SAE paper 921488, 1992
[9] Mingfa, Y., *et al*., Experimental Study of Multiple Injections and Coupling Effects of Multi-Injection and EGR in a HD Diesel Engine, SAE technical paper 2009-01-2807, 2009
[10] Park, C., *et. al*., Effects of Multiple Injections in a HSDI Diesel Engine Equipped with Common Rail Injection System, SAE technical paper 2004-01-0127, 2004
[11] Pierpont, D.. *et al*., Reducing Particulate and NO_x Using Multiple Injections and EGR in a D.I. Diesel, SAE paper 950217, 1995
[12] Payri, F., *et al.*, Complete 0D Thermodynamic Predictive Model for Direct Injection Diesel Engines, *Applied Energy, 88* (2011), 12, pp. 4632-4641
[13] Qi, K., *et al*., Simulation of Quasi-Dimensional Combustion Model for Predicting Diesel Engine Performance, *Appl Math Model., 35* (2011), 2, pp. 930-940

[14] Jayashankara, B., Ganesan, V., Effect of Fuel Injection Timing and Intake Pressure on the Performance of a DI Diesel Engine – A Parametric Study Using CFD, *Energ Convers Manage., 51* (2010), 10, pp. 1835-1848
[15] Mobasheri, R., Peng, Z., Investigation of Pilot and Multiple Injection Parameters on Mixture Formation and Combustion Characteristics in a Heavy Duty DI-Diesel Engine, SAE technical paper 2012-01-0142, 2012
[16] Stiesch, G., *Modeling Engine Spray and Combustion Processes*, Springer-Verlag, Berlin, 2003
[17] Ghojel, J. I., Review of the Development and Applications of the Wiebe Function: A Tribute to the Contribution of Ivan Wiebe to Engine Research, *Int J Engine Res., 11* (2010), 4, pp. 297-312
[18] Miyamoto, N., *et al*., Description and Analysis of Diesel Engine Rate of Combustion and Performance Using Wiebe's Functions, SAE International Congres and Exposition, Detroit, Mich., USA, 1985, SAE paper 850107
[19] Annand, W. J. D., Heat Transfer in the Cylinders of Reciprocating Internal Combustion Engines, *Proc Instn Mech Engnrs, 117* (1963), pp. 973-996
[20] Aithal, S. M., Modeling of NO_x Formation in Diesel Engines Using Finite-rate Chemical Kinetics, *Appl Energ., 87* (2010), 7, pp. 2256-2265
[21] Curran, H. J., *et al*., A Comprehensive Modeling Study of n-heptane Oxidation, *Combust Flame., 114* (1998), 1-2, pp. 149-177
[22] Maroteaux, F., Noel, L., Development of a Reduced n-heptane Oxidation Mechanism for HCCI Combustion Modeling, *Combust Flame., 146* (2006), 1-2, pp. 246-267
[23] Lavoie, G. A., *et al*., Experimental and Theoretical Investigation of Nitric Oxide Formation in Internal Combustion Engines, *Combustion Science and Technology, 1* (1970), 4, pp. 313-326
[24] Chase, J. M. W., *Nist-Janaf Thermochemical Tables*, American Chemical Society and the American Institute of Physics, New York, USA, 1999
[25] Nishida, K., Hiroyasu, H., Simplified Three-Dimensional Modelling of Mixture Formation and Combustion in a D. I. Diesel Engine, SAE paper 890269, 1989
[26] Petris, C. D., *et al.*, A Mathematical Model for the Calculation of Blow-by Flow and Oil Consumption Depending on Ring Pack Dynamic Part I: Gas Flows, SAE paper 941940, 1994
[27] Kolchin, A., Demidov, V., *Design of Automotive Engines* (in Russian), MIR Publishers, Moscow, Russia, 1984
[28] Borman, G. L., Ragland K.W., *Combustion Engineering*, McGraw-Hill, New York, USA, 1998
[29] Bowler, L., Throttle Body Fuel Injection (TBI) – An Integrated Engine Control System, SAE paper 800164, 1980
[30] Heider, G., *et al.*, Two-Zone Calculation Model for the Prediction of NO Emissions from Diesel Engines, *Proceedings*, 21st CIMAC Cong., Interlaken, Switzerland, 1995, pp. D52
[31] Zeldovich, Y. B., The Oxidation of Nitrogen in Combustion and Explosions, *European Physical Journal A – Hadrons and Nuclei, 21* (1946), pp. 577
[32] Baulch, D. L., *et al.*, Evaluated Kinetic Data for Combustion Modeling Supplement-I, *J Phys Chem Ref Data., 23* (1994), 6, pp. 847-1033
[33] Hanson, R. K., Salimian, S., *Combustion Chemistry*, Springer-Verlag GmbH, New York, USA, 1984
[34] Holman, J., *Experimental Methods for Engineers*, McGraw-Hill Education, New York, USA, 2011
[35] Heywood, J. B., *Internal Combustion Engine Fundamentals*, Mc-Graw Hill, New York, USA, 1988

Paper submitted: December 12, 2012
Paper revised: June 14, 2013
Paper accepted: July 4, 2013